JOURNAL OF VIROLOGY, May 1994, p. 2915–2928
0022-538X/94/$04.00+0

Vol. 68, No. 5

Distribution and Trafficking of JHM Coronavirus Structural Proteins and Virions in Primary Neurons and the OBL-21 Neuronal Cell Line

J. M. M. PASICK,† K. KALICHARRAN, AND S. DALES*

Cytobiology Group, Department of Microbiology and Immunology, University of Western Ontario, London, Ontario N6A 5C1, Canada

Received 21 October 1993/Accepted 19 January 1994

The neurotropic murine coronavirus JHM is capable of inducing various forms of neurologic diseases, including demyelination. Neurons have been shown to act as a repository site at the early stages of the disease process (O. Sorensen and S. Dales, J. Virol. 56:434–438, 1985). JHM virus (JHMV) replication and trafficking of viral proteins and virions in cultured rat hippocampal neurons and a neuronal cell line, OBL-21, were examined, with an emphasis placed on the role of the microtubular network. We show here that JHMV spread within the central nervous system occurs transneuronally and that virus protein trafficking was dependent upon microtubules. Viral trafficking occurred asymmetrically, involving both the somatodendritic and the axonal domains. Thus coronavirus can be disseminated from neurons at either the basolateral or the apical domains. A specific interaction between antibodies derived against the microtubule-associated protein tau and JHMV nucleocapsid protein (N) was observed, which can presumably be explained by an overall amino acid similarity of 44% and an identity of 20% between proteins N and tau, with optimal alignment at the microtubule binding domain of tau. Collectively, our data suggest an important role of the microtubule network in viral protein trafficking and distribution. They also draw attention to protein sequence mimicry of a cell component by this coronavirus as one strategy for making use of the host's functions on behalf of the virus.

The mechanisms by which viruses are assembled within and exit from their host cells is an important issue in virus-cell interactions. In this regard, viruses have been used as probes to address problems related to protein sorting and trafficking within cells. This has been particularly useful in cells possessing polarized membrane domains. For instance, vesicular stomatitis virus and influenza virus, which bud from basolateral and apical domains, respectively, of polarized epithelial cells (for a review, see reference 46) and the equivalent somatodendritic and axonal domains of neurons (18), do so as a result of the specific targeting of their envelope glycoproteins. Similarly, mouse hepatitis virus (MHV), a coronavirus, was used to mark the constitutive secretory pathway in AtT20 cells, a murine pituitary tumor cell line, and hence aided in determining where sorting or divergence from the regulated secretory pathway takes place in these cells (51). These types of studies are important because they are likely to provide us with a fundamental insight into how the secretory pathway in eucaryotic cells is controlled. In addition, they are likely to give us some intuitive understanding of related problems, for example, how viruses employ neurons to penetrate and spread throughout the central nervous system (CNS). With respect to the latter, we have been examining the interactions between MHV and rodent neuronal cells. MHVs of the A59 and JHM strains can invade the CNS of mice by way of the olfactory and trigeminal nerves following intranasal inoculation (5, 6, 32, 43). Accordingly, interneuronal spread was the mechanism hypothesized to account for this mode of virus penetration into the CNS. Subsequent dissemination to other CNS regions was shown to also involve specific neuronal populations and tracts (32, 44, 45). Immunohistochemical and in situ hybridization methods have shown that in mice, MHV-A59 manifests tropism toward neurons of the olfactory nuclei, nuclei of the amygdala, central tegmental nucleus, entorhinal cortex, subiculum, claustrum, lateral habenular nucleus, subthalamic nucleus, substantia nigra, and septal nuclei in addition to other sites (21, 32). In rats, JHM virus (JHMV) was shown to have tropism for hippocampal and cerebellar Purkinje neurons (36, 41, 49, 50). Assembly of JHMV and MHV-A59 virions in fibroblastic cells occurs within the perinuclear region by budding at transitional reticulum vesicles positioned between the rough endoplasmic reticulum and the Golgi apparatus (35, 52, 53). The time and location of progeny virion assembly appear to be controlled by the kinetics of integral membrane glycoprotein (M protein) deposition on these transitional vesicles (52). Similar observations were made with MHV-infected AtT20 murine pituitary tumor cells in which progeny virions were shown, as previously mentioned, to exit cells via the constitutive rather than the regulated, or induced, exocytic pathway (51). Similar phenomena have also been reported for JHMV assembly in cultured mouse spinal cord neurons (20).

The release of progeny virions to the outside in all the above examples likely involves a microtubule-dependent process. In the present study, JHMV replication and trafficking of viral proteins and virions in cultured rat hippocampal neurons and OBL-21 cells, a stable homogeneous murine cell line expressing a neuronal phenotype (47), were examined, with emphasis placed on the role of the microtubular cytoskeleton in these events.

* Corresponding author. Mailing address: Department of Microbiology and Immunology, Health Science Centre, University of Western Ontario, London, Ontario N6A 5C1, Canada. Phone: (519) 661-3448. Fax: (519) 661-3499.

† Present address: Agriculture Canada, Sackville, New Brunswick E0A 3C0, Canada.

MATERIALS AND METHODS

Viruses. MHV strain JHM, originally obtained from the American Type Culture Collection (Rockville, Md.), and the JHMV variant AT11f cord virus, which bears deletions in the coding sequences for the spike glycoprotein, S, and the hemagglutinin-esterase, HE (31, 38), were propagated and titrated on murine L-2 fibroblasts as previously described (9).

Cultures of OBL-21 cells. OBL-21 cells (47) were routinely grown on either poly-L-lysine-coated, 12-mm-diameter glass coverslips or 35-mm-diameter petri dishes (Nunc) in Dulbecco modified Eagle medium (DMEM) supplemented with 10% (vol/vol) fetal bovine serum (Hybrimax; Sigma), 15 mM HEPES (*N*-2-hydroxyethylpiperazine-*N'*-2-ethanesulfonic acid) (pH 7.3), and 10 μg of gentamicin per ml. To enhance neurite outgrowth prior to inoculation with virus, dibutryl cyclic AMP was added to the culture medium to a final concentration of 2.5 mM.

Culturing hippocampal neurons. Embryonic day 18 to 20 (E18 to E20) Wistar Furth rats were used for the preparation of dissociated hippocampal neuron cultures by the procedures described by Banker and Goslin (1), with minor modifications. Hippocampi were microscopically dissected from rat embryos and placed in ice-cold plating medium consisting of a 1:1 mixture of DMEM and Ham's F12 supplemented with 10% (vol/vol) fetal bovine serum, 15 mM HEPES (pH 7.3), and 10 μg of gentamicin per ml. The tissue was washed with ice-cold Ca^{2+}- and Mg^{2+} free phosphate-buffered saline (PBS) (pH 7.2) and then digested with 1× trypsin-EDTA (Sigma) at 37°C for 15 min. The tissue was washed twice with cold plating medium to inactivate the trypsin and then gently dissociated by repeated passage through a fire-polished Pasteur pipette. The crude cell suspension which resulted was passed successively through 130- and 33-μm-pore-size nylon meshes (Nitex) to remove large cell clumps and then layered onto a cushion of fetal bovine serum and centrifuged at 150 × *g* for 7 min. The cell pellet produced was resuspended in a small volume of cold plating medium, and the viable cell numbers were determined by counting the total cells present and trypan blue excluding cells. Cells were seeded at a density of 3×10^4 to 6×10^4 viable cells per cm^2 onto poly-L-lysine-coated, 12-mm-diameter glass coverslips, precleaned with concentrated HNO_3, or onto poly-L-lysine-coated 35-mm-diameter plastic petri dishes. Following attachment to the substratum for 2 h, the plating medium was exchanged for a serum-free neuronal medium consisting of a 1:1 mixture of DMEM and Ham's F12 supplemented with 100 μg of transferrin per ml, 5 μg of bovine insulin per ml, 100 μM putrescine, 20 nM progesterone, and 30 nM sodium selenite (11) with the addition of 1 mM sodium pyruvate. To promote viability of hippocampal neurons, they were cocultured in the presence of type 1 astrocytes, which provided trophic support and countered the neurotoxic effects of the excitatory amino acid neurotransmitter glutamate. For coculturing, astrocytes were attached to the surface of 60-mm-diameter petri dishes while neurons were placed on 12-mm-diameter glass coverslips. Another procedure involved placing the astrocytes on 24.5-mm-diameter, collagen-coated Costar transwell inserts with 0.4-μm pores (catalogue no. 3425) and the neuronal cultures onto the surface of Costar six-well cluster plates, as described by Walsh et al. (59). The cells were maintained in a humidified atmosphere at 37°C with 5% CO_2. Approximately one-third of the culture medium was exchanged every third day.

Infection of neuronal cultures with viruses. Primary hippocampal neuronal cultures growing on coverslips were removed from the dishes in which they were being cocultured with type 1 astrocytes, transferred to new dishes, and then inoculated with either wild-type (wt) JHMV or the AT11f cord virus variant at a multiplicity of infection (MOI) of between 5 and 30 PFU per cell in 70 to 90 μl. Hippocampal neurons growing on plastic in 35-mm-diameter dishes were inoculated with virus by first removing the transwell insert containing the type 1 astrocytes and then aspirating the culture medium and inoculating at MOIs as described above in a volume of 400 μl. Adsorption was carried out for 60 min in a 5% CO_2 incubator at 37°C with intermittent gentle rocking to facilitate the uniform spread of virus over the surface of the 35-mm-diameter dishes. Following virus attachment, cultures were washed twice with Hanks' balanced salt solution and then placed in neuronal medium as described above and cocultured with type 1 astrocytes. OBL-21 cultures growing on either 12-mm-diameter glass coverslips or in 35-mm-diameter petri dishes were inoculated with virus by a similar procedure, using MOIs of 1 to 10.

Vinblastine treatment of OBL-21 cultures. Vinblastine sulfate (David Bull Laboratories, Melbourne, Australia) was added to a final concentration of 10 μg/ml at either 24 or 36 h following inoculation with JHMV for cultures used in the electron microscopic evaluation of the microtubular network in MHV assembly and release. Vinblastine was added to a final concentration of 5 μg/ml at 6 h postinoculation in experiments designed to assess the influence of the microtubular network on the kinetics of virus growth and release from OBL-21 cells.

Immunostaining of neuronal cultures. Immunocytochemical labelling of primary hippocampal neuron and OBL-21 cultures by indirect fluorescent-antibody technique was done as described previously (42). Prior to the application of antibodies, cells were fixed either in 4% paraformaldehyde in PBS for 5 min and then permeabilized by exposure to acetone for 30 s or in 4% paraformaldehyde plus 0.25% glutaraldehyde for 10 to 15 min followed by immersion in graded 50, 70, and 95% ethanol solutions before permeabilization for 30 min in 95% ethanol as described by Caceres et al. (12). Similar results were obtained with the two methods. Primary antibodies were diluted in PBS at pH 7.2 containing 3% (wt/vol) bovine serum albumin as follows: cell-specific rabbit anti-tau serum (T-6402; Sigma), 1:100; rabbit antitubulin serum (40), 1:40; monoclonal antibody (MAb) against the 160-kDa subunit of neurofilaments as tissue culture supernatant (Amersham), 1:5; rabbit antibodies against bovine glial fibrillary acidic protein (GFAP) (Dakopatts, Glostrup, Denmark), 1:40; JHMV-specific MAb 5B-170 and 5B-19.2 ascites fluid against S protein, 1:10, and MAb 4B6.2 culture supernatant against N protein, 1:8 (all generously provided by M. J. Buchmeier, The Scripps Research Institute). Fluorochrome-conjugated secondary antibodies were diluted with PBS 1:30 for goat anti-mouse immunoglobulin G-fluorescein isothiocyanate (FITC) (Sigma) and 1:50 for goat anti-rabbit immunoglobulin G (heavy and light chains)-Texas Red (Jackson Immunoresearch Laboratories).

FIG. 1. Assessment of the compartmentalization of JHM virions in OBL-21 neuronal cells by ultrastructural studies. Thin sections of infected OBL-21 cells were examined by electron microscopy to assess JHMV maturation. (A) Linear array of progeny virions found within cisternae of infected OBL-21 cells. M, mitochondria. (B) Higher magnification of the area shown in panel A. (C) Virions associated with microtubules within vesicles. Arrows point towards microtubules. Bars = 0.5 μm.

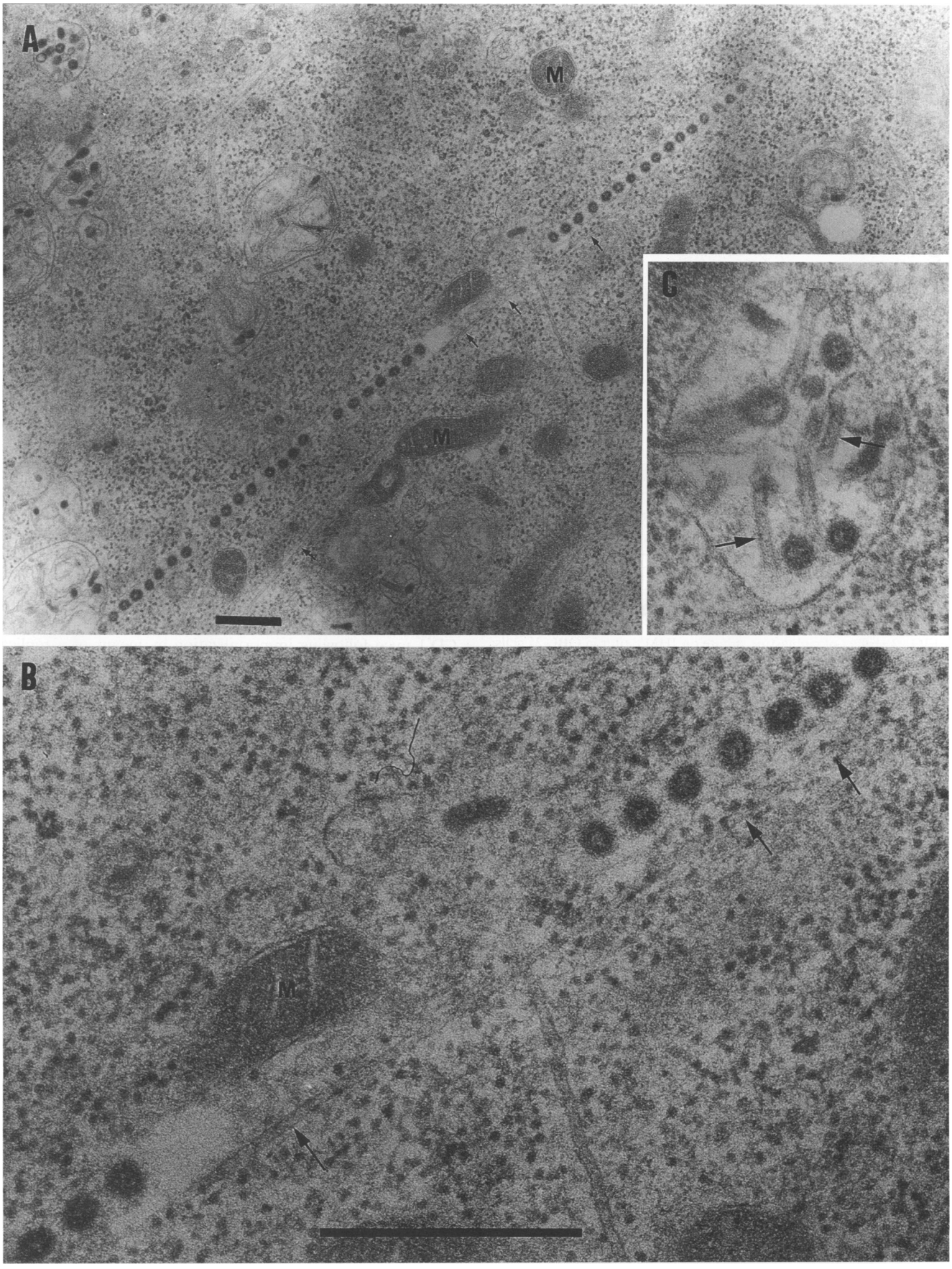
A
M
M
C
B
M

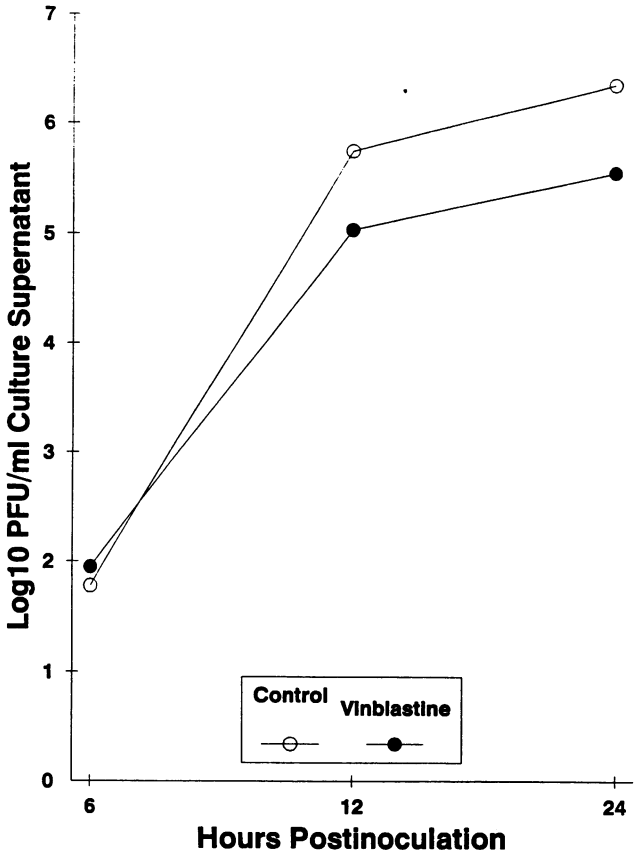

FIG. 2. Effect of vinblastine sulfate on JHMV titer in OBL-21 cells. Cultures were treated with vinblastine sulfate and infected as described in Materials and Methods. Supernatant was collected at the indicated times and assayed for PFU per milliliter.

Electron microscopy of monolayer cultures. JHMV-infected and uninfected primary hippocampal and OBL-21 monolayer cultures situated in 35-mm-diameter petri dishes (Corning) were prepared for electron microscopy as previously described (42). Cultures were washed with 0.1 M sodium phosphate buffer (pH 7.0) and then fixed in situ for 5 min with 1% (vol/vol) glutaraldehyde in 0.1 M sodium phosphate buffer. Following fixation and three washes with 0.1 M sodium phosphate buffer, cells were postfixed with 1% (vol/vol) OsO_4 in sodium phosphate buffer, dehydrated by using a series of graded ethanol solutions, and embedded in epoxy resin. Sections were cut parallel to the plane of the attachment surface, stained with uranyl acetate and then lead citrate, and viewed in a Philips EM 300 electron microscope.

Immunoblotting. OBL-21 cells were infected with JHMV at an MOI of 10 for 60 min at 4°C. The unattached viral inoculum was aspirated, and the cells were washed three times with cold PBS. Warm growth medium was added, and the cells were incubated at 37°C. After 6 h, 10 μg of vinblastine sulfate was added and the cells were reincubated for an additional 8 h. The growth medium was aspirated, and an equivalent amount of cell material was dissolved into gel loading buffer (0.063 M Tris-HCl, 2% sodium dodecyl sulfate [SDS], 10% glycerol, 5% mercaptoethanol, 0.01% bromophenol blue).

Samples were resolved in an SDS–10% polyacrylamide gel (29). Proteins were transferred from the gel to a nitrocellulose membrane overnight at 4°C at 35 mV (54). The transfer buffer contained 0.025 M Tris-HCl, 0.192 M glycine, and 20% methanol, with SDS left out to promote renaturation. The membrane was blocked with PBS containing 0.2% Tween 20 for 2 h, then probed for 2 h with either anti-N (1:1,000; 4B6.2) or anti-S (1:1,000; 5B-170) MAb, and washed three times with PBST, and binding was detected with ^{125}I-rabbit anti-mouse kappa chain immunoglobulin G.

Purification of N protein was done as described by Mohandas and Dales (37) with the exception that ^{32}P labelling was not included. For the immunoblot involving the purified JHMV N proteins, samples were electroblotted onto a nitrocellulose membrane from an SDS–10% polyacrylamide gel. Strips of membrane were probed with MAbs against N and both MAb (1:1,000) and polyclonal antibodies (1:100) against tau (Sigma). The binding was detected as described above.

RESULTS

Compartmentalization of virus components and whole virions within OBL-21 neuronal cells. The continuous neuronal cell line OBL-21 was employed to assess the putative importance of microtubules in movement and release of progeny virions to the cell exterior. This cell line, which is permissive for JHMV, was clonally derived from olfactory bulb cultures of CD.1 mice following immortalization by means of a replication-defective retrovirus vector encoding the avian *myc* gene (47). Cells of the OBL-21 line have exhibited a stable, homogeneous neurofilament-positive and GFAP-negative phenotype during culture in this laboratory and possess other neuronal characteristics, such as voltage-dependent potassium channels (47). Electron microscopic and immunofluorescence analyses of JHMV-infected OBL-21 cells demonstrated the distribution of N and S components to neurite-like processes, paralleling the findings observed with infected neurons in primary rat telencephalic cultures (42). Examination of thin sections by electron microscopy often revealed nucleocapsid aggregates in the vicinity of microtubules, as was originally observed in infected primary neurons (42). Virions organized in precise linear arrays, evident within cisternae sometimes contiguous to microtubules, were often found in favorably oriented thin sections (Fig. 1A and B). To identify the specificity of the virus-microtubule relationship more clearly, JHMV-infected OBL-21 cells were treated with vinblastine. Vinblastine, a mitotic inhibitor which also inhibits axonal transport, promotes microtubule depolymerization and the subsequent reorganization into massive tubulin paracrystals (8, 17). The objectives of treating infected OBL-21 cultures with this drug were to assess its effects (i) on the kinetics of virus

FIG. 3. Ultrastructural studies of infected OBL-21 cells assessing the effects of vinblastine sulfate. (A) Note the presence of concentrated helical nucleocapsids (N) within the cytosol. Numerous budding and progeny virions are evident within vesicles of the smooth endoplasmic reticulum which are in contact with tubulin paracrystals (PC) (arrows). (B) Higher resolution of concentrated nucleocapsids. (C) Association of N with longitudinally oriented group of microtubules. (D) Example of the close interaction of N with PC (arrows) shown at a higher magnification. (E) Budding of virions into the lumen of a vesicle (arrow). (F) Virions present in Golgi membranes in the vicinity of PC. Bars: A to D and F, 0.5 μm; E, 0.25 μm.

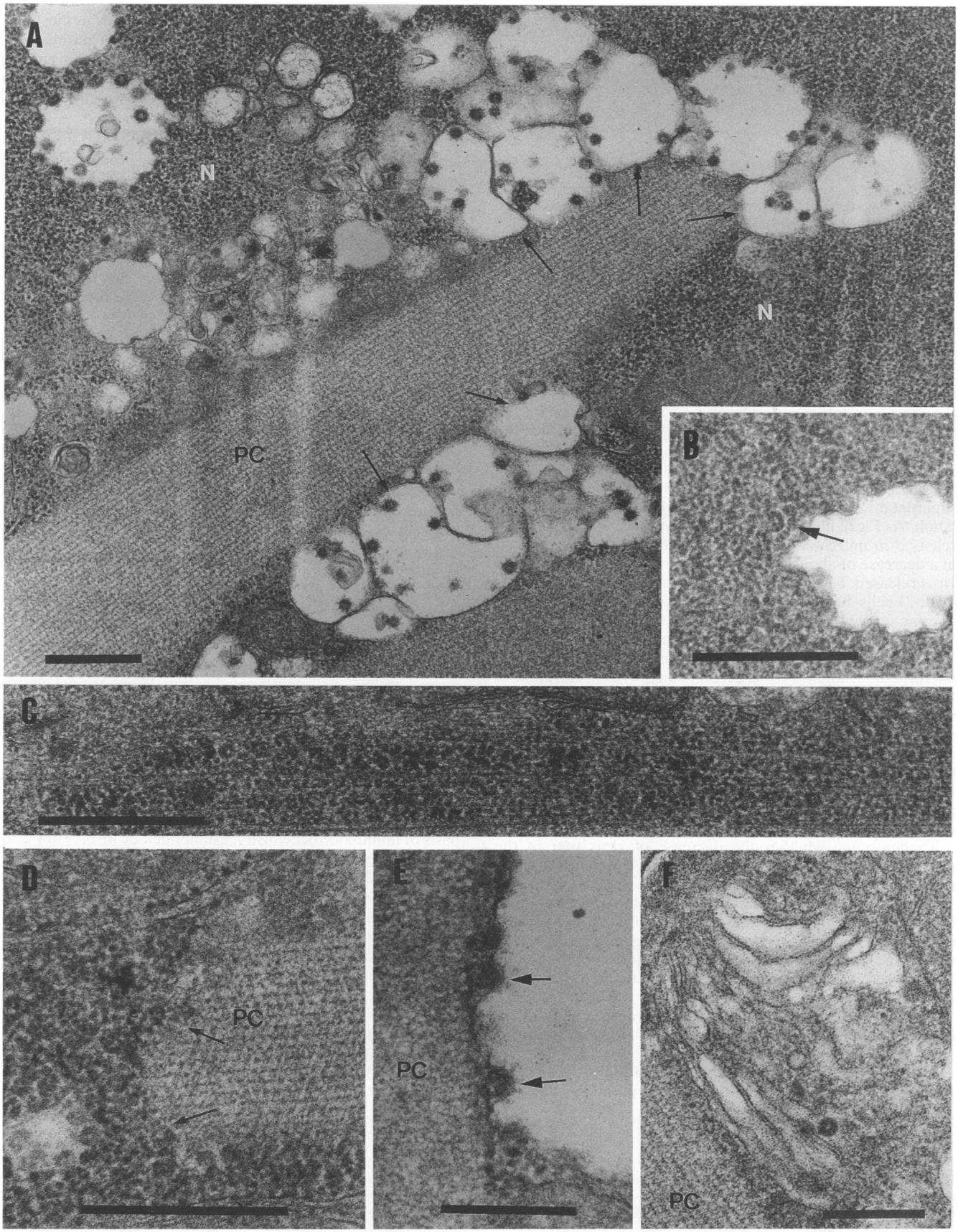
A
N
N
PC
B
C
D
PC
E
PC
F
PC

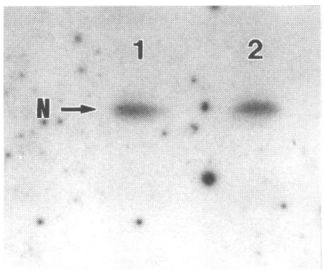

FIG. 4. Western blotting (immunoblotting) analysis of virus-specified synthesis in the absence and presence of vinblastine sulfate. Equal amounts of untreated and treated JHMV-infected OBL-21 cells were processed for immunoblotting using MAb against N. Lane 1, untreated cells; lane 2, cells in the presence of 10 μg of vinblastine sulfate per ml.

growth and release into the culture supernatant and (ii) on virion assembly as evident at the ultrastructural level. OBL-21 cultures were inoculated with JHMV at an MOI of 3, washed three times, and incubated for 3 h to allow internalization of the inoculum before neutralization of any virus remaining at the surface, using anti-S MAb 5B-19.2 diluted 1:60. Once the neutralizing antibody was washed away, vinblastine sulfate was added to half of the cultures at 6 h postinoculation. To assess the effects of vinblastine treatment on virus release, the supernatant was assayed for PFU at 6, 12, and 24 h postinoculation. As Fig. 2 illustrates, compared with the amount of virus released in untreated cultures, vinblastine treatment resulted in a decrease of about an order of magnitude in the amount of virus released. Effects on the ultrastructure of JHMV-infected OBL-21 cells due to treatment with 10 μg of vinblastine per ml became evident beginning at 12 or 18 h postinoculation. The drug effects were more pronounced during incubation for an additional 6 to 12 h (Fig. 3). The observed collapse of the microtubule framework was accompanied by concentration of viral nucleocapsid assembles within the cytosol and of progeny virions within the smooth endoplasmic reticulum and Golgi vesicles. Both nucleocapsids and virus-containing vesicles were in close contact with tubulin paracrystals (Fig. 3A, B, and D through F). These observations point to the important role that microtubules may play in the intracellular distribution and perhaps transport of nascent viral material and progeny particles.

To determine whether the decrease of virus titer in the supernatant of vinblastine-treated cells was due to inhibition of synthesis by the drug or interruption of virus release caused by disruption of the microtubule network, a comparison was made by immunoblotting equal amounts of vinblastine-treated and untreated cell extracts. As evident from Fig. 4, the addition of vinblastine (lane 2) did not affect synthesis of N protein. Similar results were obtained after immunoblotting for S protein (data not shown).

Taken together, these observations imply that microtubules may have an essential function in viral protein trafficking and/or assembly.

Virus replication and compartmentalization of virus progeny and viral components in primary hippocampal neurons. Primary rat hippocampal neurons were compared with OBL-21 cells with regard to their ability to function as hosts for JHMV synthesis, assembly, and dissemination. Cultures were prepared by using hippocampi from E18 to E20 rats according to the outline in Materials and Methods. Within 6 h after plating, many of the neurons commenced sprouting neurites which continued to extend so that by 24 h most cells possessed one long and several short neurites emanating from their soma (Fig. 5A), as described by Dotti et al. (19). The short processes have been identified as dendritic precursors while the single, long process was shown to be the presumptive axon (2, 3, 12, 19). After 1 week in culture, many of the neuronal cell bodies aggregated to form small clusters while the extended neurites formed a fine meshwork which covered the substratum. Fasciculation of axons was particularly prominent in cultures seeded at the higher cell densities (Fig. 5B). The number of contaminating astrocytes inevitably introduced along with neurons varied between preparations, usually not exceeding 40% of the total cell population (Fig. 5C). Although these primary dissociated cultures were evidently not pure, they were nevertheless highly enriched. Under these conditions, neuronal cell viability could be routinely maintained for 2 to 3 weeks.

Hippocampal neurons such as those apparent in Fig. 5A were inoculated with JHMV between 9 and 11 days in vitro at MOIs of 5 to 30 PFU per cell. At the time of virus challenge, most axons and dendrites were expected to have reached a mature state, in terms of their organization, function, and ability to form synapses (1). For comparison with wt JHMV, two isolates, AT11f cord (38) and V5A13 (23) (provided by M. Buchmeier), with altered antigenic and pathogenic properties in vivo were also employed. AT11f cord and V5A13 viruses possess deletions within the S1 portion of the S gene (23, 31). These variants were of particular interest to us because of their reported attenuation in neurovirulence, based on the shift in the pattern of disease induced from that of a fatal encephalomyelitis to one of chronic demyelination. Hippocampal neuron cultures could support growth of both wt and variant viruses (Table 1), although the titers produced were never as high as those observed with OBL-21 cells. Interestingly, as evident from Table 1, the AT11f cord and V5A13 variants grew generally better than wt JHMV and for this reason were included for comparison. However, no differences in neuronal pathology between the wt and variants were evident. On the basis of immunocytochemistry, exemplified by images in Fig. 6, approximately 1% of the cells were scored as virus antigen positive at 24 h postinoculation. Although the frequency of infected cells increased with time, it remained low, even 5 days after inoculation. This was in contrast to the situation observed at 24 h postinoculation with JHMV-infected OBL-21 cultures, in which about half of the cells became virus antigen positive. In some neuronal cultures, astrocytic elements of undetermined lineage represented as a significant fraction of all cells (Fig. 6B, D, and F). The astrocytic cells did not usually manifest any infection prior to 48 h postinoculation, in agreement with previous observations with mixed telencephalic cultures (42). When infection did occur, the astroglia involved became part of the syncytial formation (Fig. 6F), in contrast to

FIG. 5. Primary hippocampal neurons in culture. Hippocampi were dissected at E18 to E20 as described in Materials and Methods. (A) Phase-contrast micrograph of a low-density culture at 10 days in vitro illustrating long prominent axons (arrows). (B) Culture seeded at a higher density than for panel A and labelled with a MAb against 160-kDa neurofilament protein. Note the neuritic network with a prominent axonal fascicle (arrows). (C) Same field as in panel B but labelled with a rabbit polyclonal antibody against GFAP, demonstrating the presence of astrocytes in the culture. Bars = 20 μm.

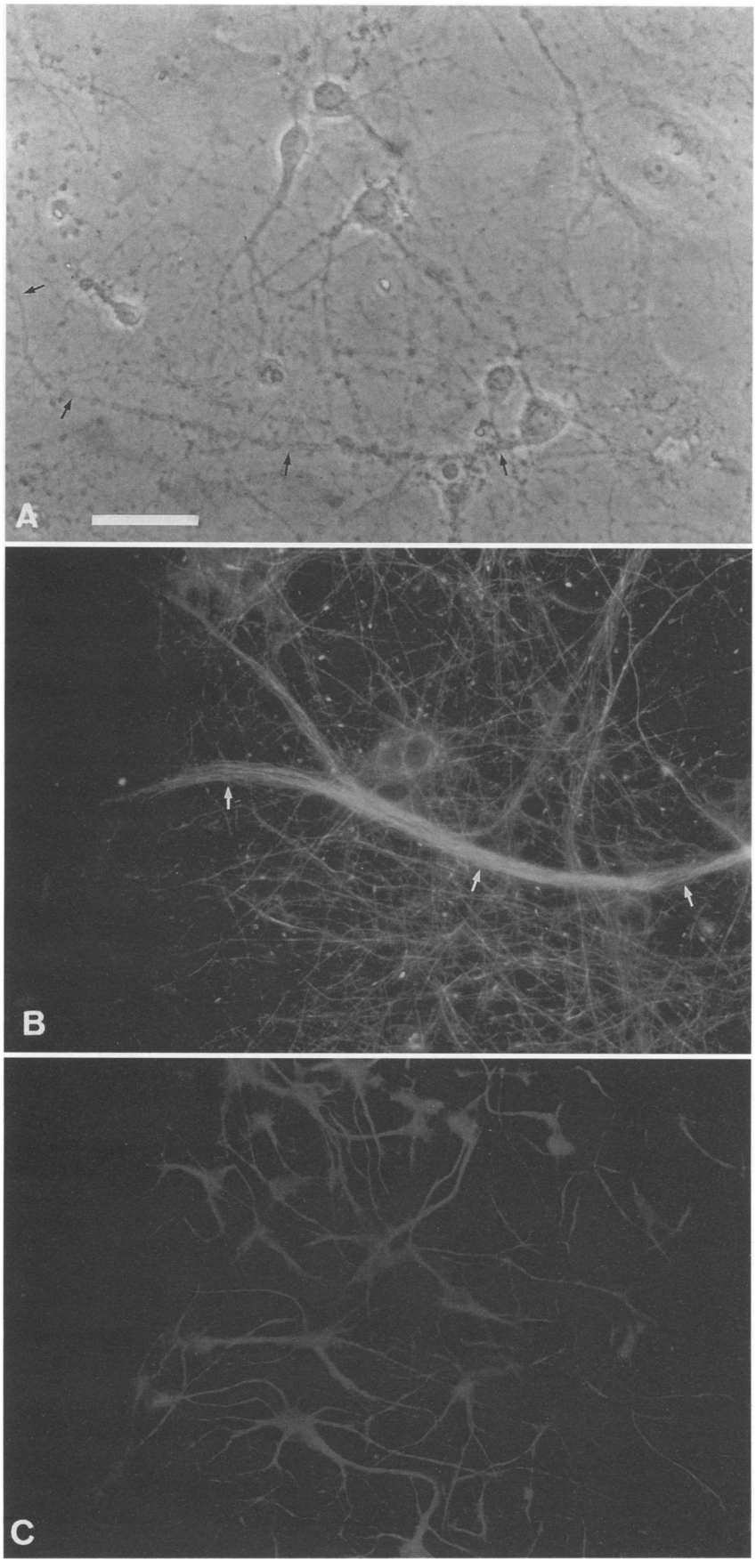
A
B
C

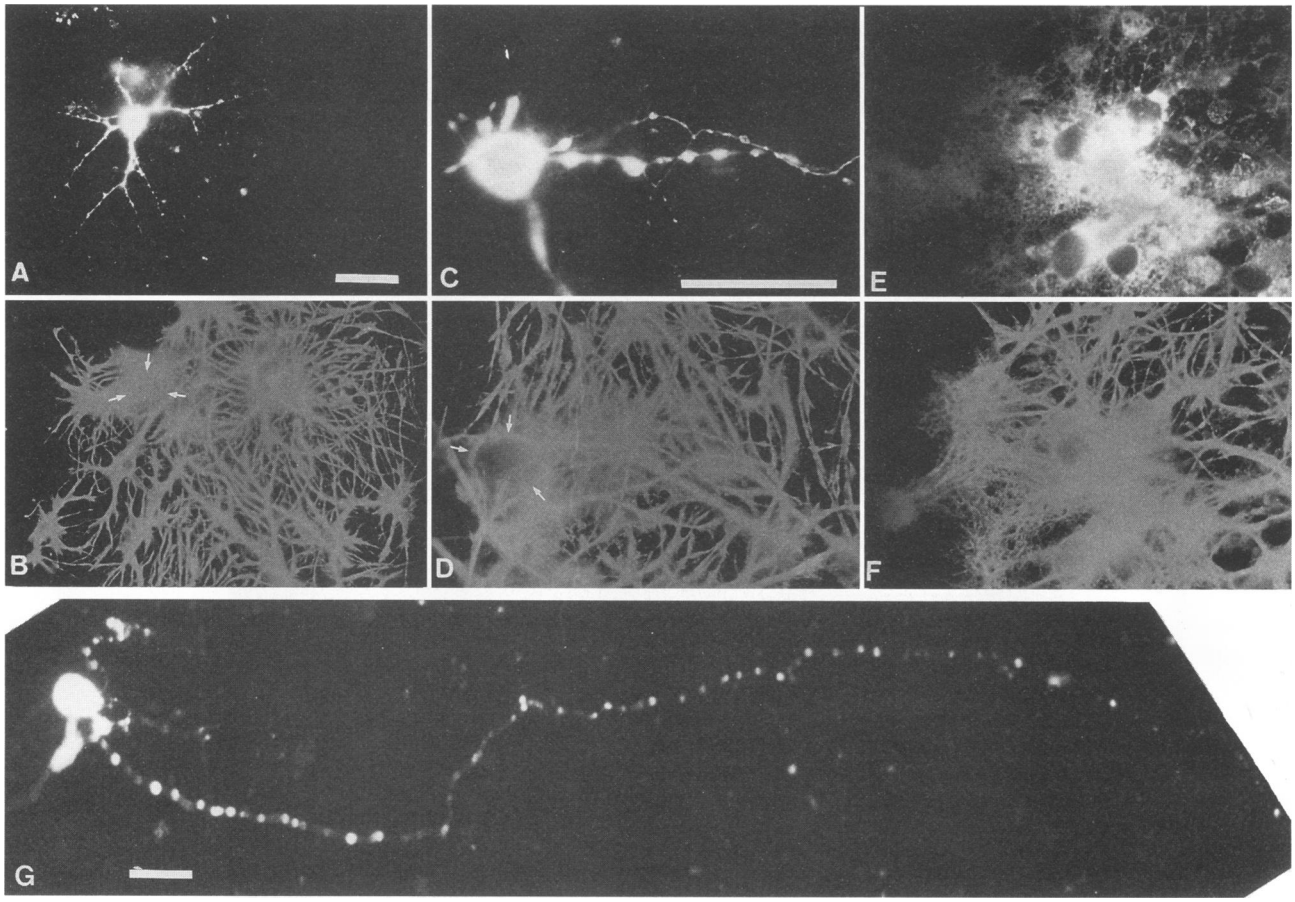

FIG. 6. Identification of JHMV-infected cells in cultures of hippocampal neurons. Infected astrocytes were detected by dual labelling with sera against GFAP and N, while infected neurons were identified on the basis of morphology and staining of N in the absence of GFAP staining. The same areas are shown in panels A and B, C and D, and E and F. Arrows in panels B and D, positions of neurons shown in panels A and C, respectively. Cells were labelled for the presence of protein N in panels A, C, E, and G and labelled for GFAP in panels B, D, and F. Note the presence of N at the soma and neurites in panels A, C, and G. Bars = 10 μm.

neuronal infections in which syncytiogenesis was not evident (Fig. 6A, C, and G).

Immunocytochemistry and electron microscopic studies of thinly sectioned neurons were used to localize JHMV particles and components. N and S antigens were present in tapering, short neurites or presumptive dendrites as well as in highly extended, fine axonal processes. Dual immunolabelling of viral and cytoskeletal antigens with antibodies specific for N, S, or tau (Fig. 7 and 8) provided some understanding of the process by which viral proteins became localized in relation to the two cytoskeletal domains. tau and MAP2 are two microtubule-associated proteins which participate in formation of cross bridges between adjacent microtubules (24). In cultured rodent neurons, tau and MAP2 become segregated to predominantly axonal and somatodendritic domains, respectively (26), corresponding to their distribution within the CNS (10). However, the topographical separation of tau and MAP2 in cultured hippocampal neurons is not absolute. During establishment of the cultures, MAP2 and tau are codistributed within presumptive axonal and dendritic neurites (12, 26); this may occur because in vitro axons usually originate from the proximal segment of a branching dendrite, contrary to the in vivo situation, in which axons develop as an autonomous projection emanating from the cell soma (7). In neuronal cultures such as that in Fig. 7, prominent axonal fasciculation was apparent. Dual presence of tau with JHMV-specified N or S protein was evident in axon-like neurites (Fig. 7A versus B; Fig. 8A versus B and C versus D). This result supports other evidence for the occurrence of viral protein trafficking within these domains. Electron microscopic examination of thinly sectioned hippocampal cultures revealed the close association of JHMV nucleocapsid helices with bundles of microtubules (Fig. 9A), confirming our previous finding with neurons present in stratified, mixed telencephalic cultures (42). Occasionally, entire virions were evident inside vacuoles within neurites (Fig. 9B).

A highly plausible explanation which can account for the presence of nucleocapsids in the vicinity of neuronal microtubules comes from the uncovering of informational homology between the amino acid sequences of N protein and tau, illustrated in Fig. 10A. Overall, the two proteins possess a 42% similarity and 20% identity of amino acid sequences, as determined for us by Michael Clarke, Department of Microbiology and Immunology, University of Western Ontario, using the nucleotide sequence of N (49) to search the GenBank data base. When optimal alignment was made between the reported microtubule-binding repeat motif of tau (see reference 24 for a review) and residues 328 to 340 of protein N within the carboxyl-terminal portion of N by using the MACAW program (Multiple Alignment Construction and Analysis Workbench)

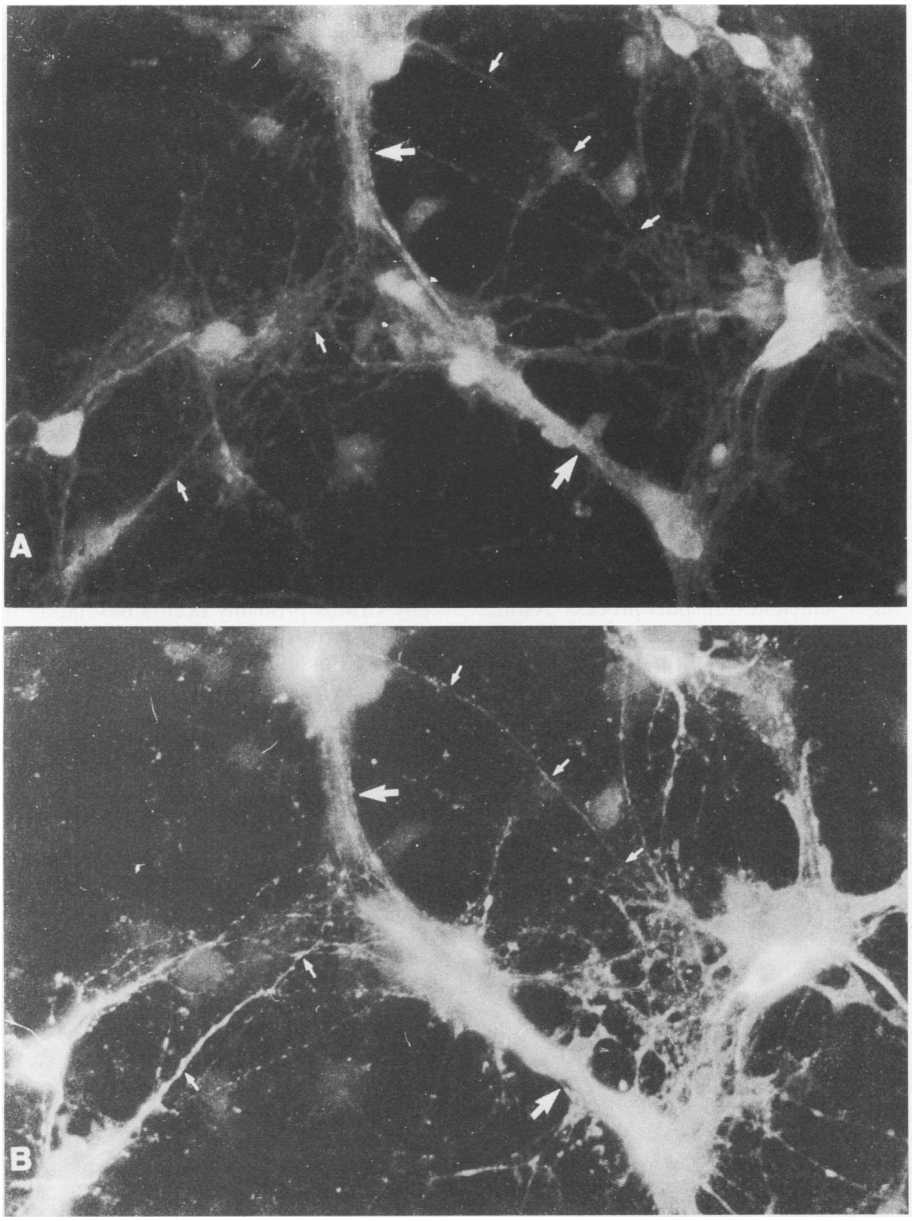

FIG. 7. Demonstration of JHMV-specific proteins within single axon-like neurites (small arrows) and fascicles (large arrows). (A) Hippocampal neuronal culture 24 h after infection with V5A13 at 10 days in vitro labelled with rabbit polyclonal antibodies against tau and Texas red-conjugated secondary antibodies. (B) Same area as in panel A but labelled with anti-S MAb and FITC-conjugated secondary antibodies. Bar = 10 μm.

(48), the comparison was found to be highly significant (P = 5.0 e-002) (Fig. 10B).

Immunoblotting was used to determine whether sequence homology between N and tau proteins is reflected in immunological recognition. For this purpose, the purified N component bound to nitrocellulose was reacted with anti-tau antibodies. Probing with MAbs against protein N confirmed the antigen identity, as shown in lanes 1 and 2 of Fig. 11. Immune cross-reactivity against N was tested with both a MAb and polyclonal rabbit antiserum against tau. It is evident from lanes 3 and 4 of Fig. 11 that both anti-tau antibodies recognized the N protein, albeit with a lower intensity in the case of the MAb. These results provided evidence for sequence and immunological relatedness between the viral and cytoskeletal proteins which might explain the interaction of both N protein and tau with the microtubules.

DISCUSSION

To understand JHMV assembly and release in neurons, one must consider the organization of these highly specialized asymmetric cells. Dendrites and axons, the two types of neurites extruded from neurons, perform specialized functions, axons being involved in conductance of electrical impulses away from the cell soma, while the multiple dendrites receive and transmit to the cell external signals. Polarization of impulse conductance by axons versus dendrites is inherent in the composition and fine structure of these appendages, which

TABLE 1. Growth of wt JHMV and S deletion variants in dissociated hippocampal neuron cultures

Expt	Virus	10^2 PFU/ml of culture supernatant (mean ± SD) at postinoculation day:				
		1	2	3	4	5
1[a]	wt JHMV	1.6 ± 0.5	4.4 ± 2.0	12.6 ± 8.0	47.0 ± 12.7	55.5 ± 17.7
	AT11f cord	3.1 ± 0.1	33.0 ± 12.1	116.0 ± 26.5	485.0 ± 57.3	239.7 ± 37.9
	wt JHMV	0.2 ± 0.2	<0.1	0	0.6 ± 1.0	1.4 ± 2.4
2[b]	AT11f cord	1.6 ± 1.0	3.3 ± 1.2	2.1 ± 1.0	15.8 ± 9.7	42.3 ± 2.3
	V5A13	4.1 ± 1.1	12.0 ± 6.2	16.6 ± 6.1	48.7 ± 22.6	79.0 ± 9.0

[a] Cells dispersed from E20 Wistar Furth rat hippocampi were seeded at a density of 60,000 viable cells per cm^2. At 11 days in vitro, cultures were inoculated with virus at an MOI of 5 PFU per cell.

[b] Cells dispersed from E20 Wistar Furth rat hippocampi were seeded at a density of 30,000 viable cells per cm^2. At 10 days in vitro, cultures were inoculated with virus at an MOI of 30 PFU per cell.

differ with respect to their membrane proteins and cytoskeletal organization (58). Conversely, alternate functions depend on the polarized distribution of proteins and organelles within these cells (see reference 46 for a review). Since biosynthetic events of neurons are generally confined to the somatodendritic domain, movement of materials to and from the apical, i.e., axonal, domain, which can extend for over a meter in length, depends on a highly efficient transport process. Axonal transport is accomplished by two microtubule-dependent processes: fast transport of membranous organelles and slow transport of cytosolic proteins, especially those of the cytoskeleton (58).

The disposition of JHMV components and progeny virions within primary hippocampal neurons and OBL-21 cells is consistent with the idea that spread of the infection within the CNS is transneuronal. Concerning the specificity of JHMV externalization, in polarized ependymal cells release of progeny virions probably occurs basolaterally, judging by the pattern of virus spread to adjacent ependyma and subependymal tissues. Possible exit from the apical ependymal surface has

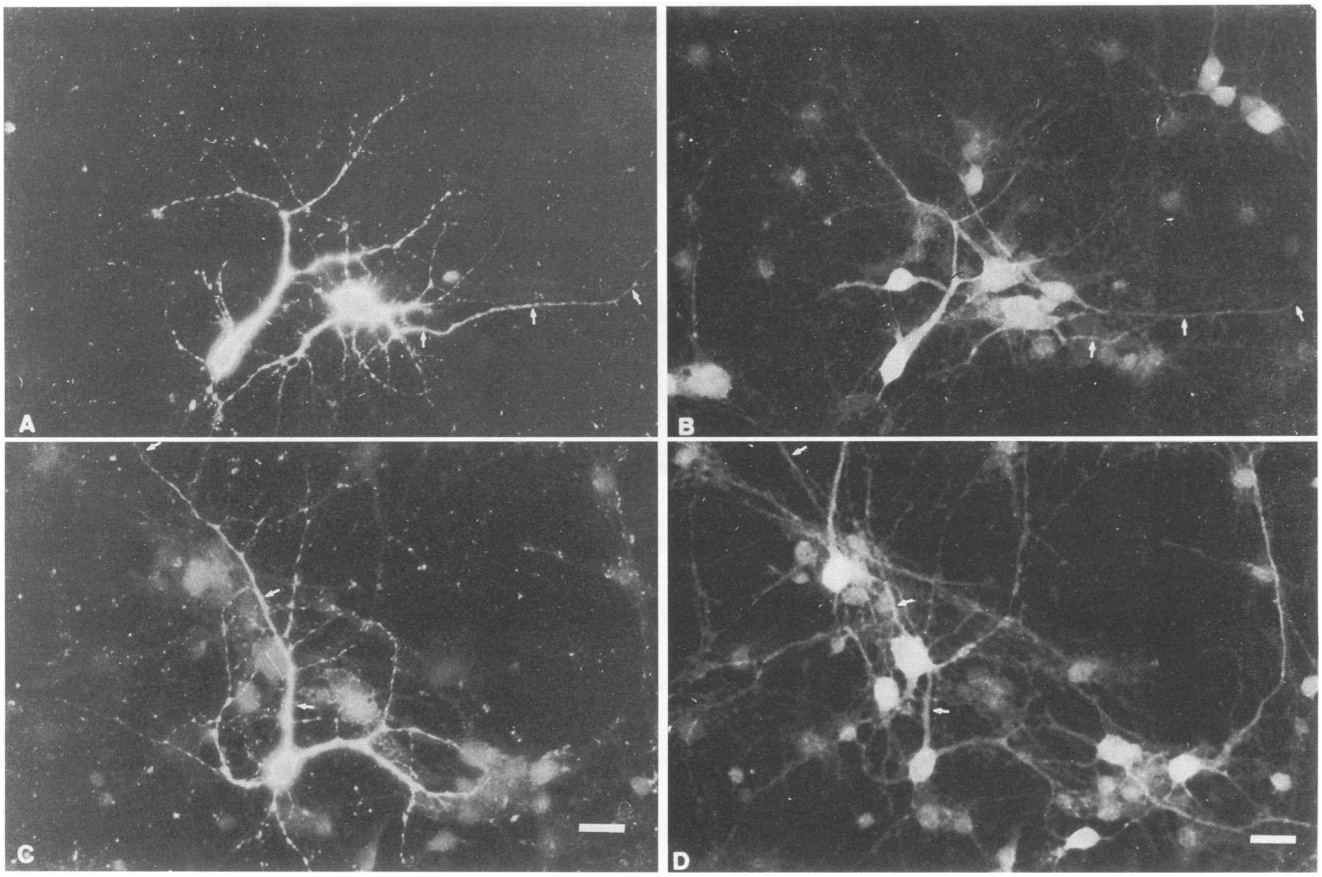

FIG. 8. Localization of V5A13 viral proteins to the two neuronal domains. E20 infected hippocampal neuronal cultures were identified immunocytochemically at 1 day postinoculation. (A) Infected neurons labelled with anti-N antibodies and FITC-conjugated secondary antibody. (B) Cells in the same field as in panel A labelled with a rabbit polyclonal antiserum against tau and Texas red-conjugated secondary antibody. (C) An infected neuron identified by using anti-S MAb and FITC secondary conjugated antibody. (D) The same field as in panel C but labelled with anti-tau as described for panel B. Arrows indicate prominent neurites. Bar = 10 μm.

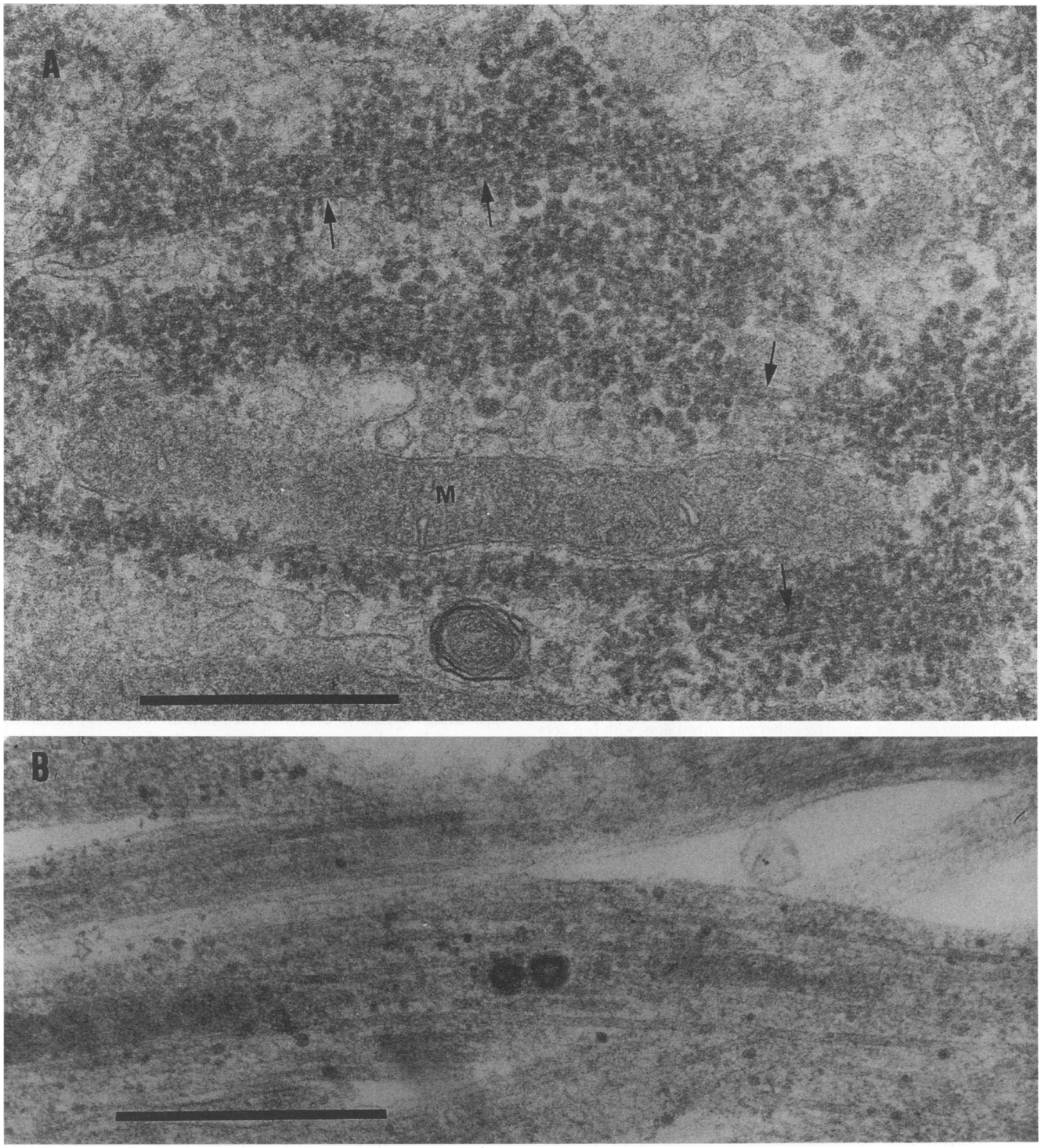

FIG. 9. Association of nucleocapsids and whole virions with microtubules within hippocampal neuron, evident by electron microscopy. (A) Accumulation of the nucleocapsid helical cores around microtubules (arrows). M, mitochondrion. (B) Presence of whole virions within a neurite. Bars = 0.5 μm.

not, however, been disproved (60). The patterns of N- and S-protein distribution in hippocampal neurons indicate that trafficking of viral components occurs somatodendritically, confirming previous observations by Knobler et al. (25) and Dubois-Dalcq et al. (20). Such vectorial movement is conceivable because elements of the Golgi apparatus, known to play a role in coronavirus assembly and transport (35), are present within dendrites (18). Coincident patterns of viral protein N, S, and tau distribution within axon bundles as well as in extremely extended neurites with axonal morphology further support the

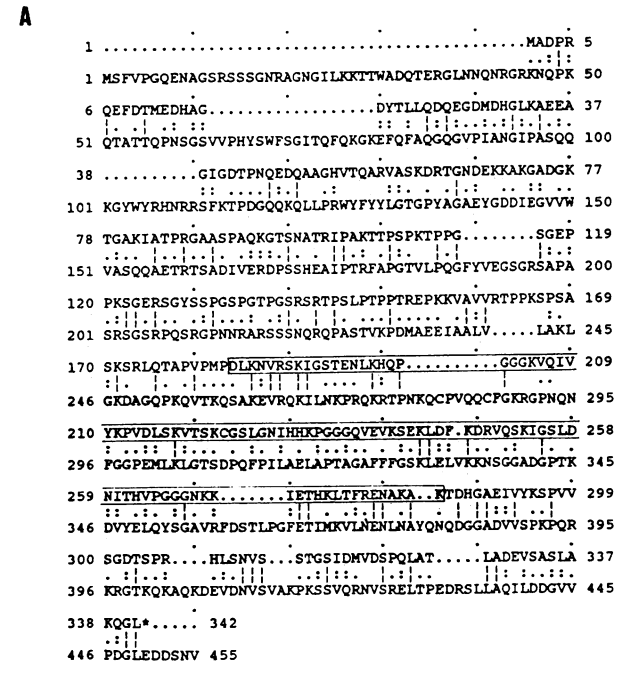

FIG. 10. Evidence for amino acid sequence homology between tau and N. (A) Optimal alignment between entire amino acid sequences of the two proteins. Identical amino acids are linked by vertical lines; related amino acids are linked by either one or two dots, with two dots designating a closer homology. Tandem repetitions in the tau sequence involved in binding with microtubules are boxed. (B) Invariant 12-mer constituting the core of tau's microtubule binding motif matched with N sequence from the carboxyl terminus.

use by JHMV of axonal trafficking. This evidence for dissemination of coronaviruses from the basolateral and/or apical domains of neurons should be contrasted with reports on the selective release at a single domain of other enveloped RNA viruses from polarized cells (18, 27, 46, 61).

Herpes simplex virus, rabies virus, and reoviruses can invade the CNS by a microtubule-dependent process of fast axonal transport. Herpes simplex virus spreads throughout the CNS by retrograde, transneuronal transfer (57), and rabies virus is disseminated by either predominantly retrograde movement (14, 28) or by retrograde and anterograde transport (30, 55), which is inhibitable by the microtubule-disrupting colchicine (13). Treatment with this drug can also disrupt reovirus type 3 bidirectional, transneuronal penetration into the CNS (22, 39, 56). From in vivo studies in which temporally related, progressive penetration and spread of JHMV within the murine CNS were traced after intranasal inoculation (4, 43), it was found that JHMV transfer along the neural pathways was predominantly retrograde, although some anterograde movement also occurred.

Evidence of an association between protein N and neuronal microtubules, established previously with mixed telencephalic cultures (42) and confirmed here in hippocampal neurons and OBL-21 cells, provides another instance of virus-microtubule

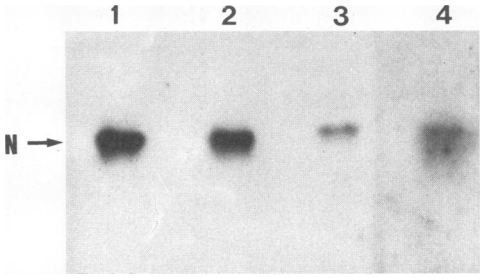

FIG. 11. Immunoblot demonstrating cross-reactivity of protein N with anti-tau antibodies. Purified N was probed with two MAbs against N (lanes 1 and 2) or with MAb and polyclonal antibody against tau (lanes 3 and 4).

interactions, demonstrated previously with reovirus type 3 (15) and adenovirus type 5 (16), drawing attention to the parasitic nature and evolution of viruses. One may suppose that by making use of the host's structure-function properties in the manner exemplified here, the viral evolutionary homolog can mimic a fundamental cell process on behalf of the virus. This association may occur as the consequence of the existence of an amino acid sequence through which protein N can recognize and become attached to the microtubules, an idea supported by the existence of a homology between proteins N and tau. The tau-microtubule linkage occurs through a 31- or 32-amino-acid sequence, which is tandemly repeated three or four times within the carboxyl-terminal segment of the molecule (33). Each repeat of tau is an 18-mer stretch, which can bind to microtubules as an isolated peptide (34). Among the repeats, 12 of the 18 invariant residues (24) could be aligned optimally with residues 328 to 340 of protein N (Fig. 10B), thus providing suggestive evidence for possible homology in attachment of N and tau to microtubules and offering a hypothesis amenable to experimental verification. Immunological recognition of protein N by anti-tau antibodies (Fig. 11, lanes 3 and 4) strengthens this hypothesis. The relationship between N and microtubules may have further implications for progeny virion assembly. One could consider the protein N-microtubule association as a significant step in virion assembly, whereby cytosolic protein N when present on microtubule surfaces becomes relevantly positioned for subsequent interaction with the integral membrane glycoprotein M during the process of budding into vacuoles. Such a sequence of events could account for the observed linear distribution of virions within membranous cisternae of OBL-21 cells, in which adjacent microtubules are also evident. It remains to be established whether nucleocapsids not utilized for incorporation into progeny coronavirions are transferred into neurites by a slow axonal transport mechanism generally held to be responsible for the movement of cytoskeletal components into axons (58). This could explain the observed association between nucleocapsid cores and the extended microtubule arrays of neurites. Further understanding of these phenomena will likely contribute significantly to our understanding of both protein trafficking and coronavirus neuropathogenesis.

ACKNOWLEDGMENTS

We thank A. Hanington for expertise in maintenance of the animal colony and S. Wilton for contribution to the electron microscopy work.

This work was supported by grants from the Medical Research Council of Canada and the Multiple Sclerosis Society of Canada to S.D. J.M.M.P. was the recipient of a postdoctoral fellowship and K.K.

was the recipient of a studentship from the Multiple Sclerosis Society of Canada.

REFERENCES

1. **Banker, G., and K. Goslin.** 1991. Rat hippocampal neurons in low density culture, p. 251–281. *In* G. Banker and K. Goslin (ed.), culturing nerve cells. MIT Press, Cambridge, Mass.
2. **Banker, G. A., and W. M. Cowan.** 1977. Rat hippocampal neurons in dispersed culture. Brain Res. **126:**397–425.
3. **Banker, G. A., and W. M. Cowan.** 1979. Further observations on hippocampal neurons in dispersed culture. Comp. Neurol. **187:** 469–494.
4. **Barnett, E., and S. Perlman.** Mouse hepatitis virus and herpes simplex virus move along different CNS pathways after intranasal inoculation. Adv. Exp. Med. Biol., in press.
5. **Barthold, S. W.** 1988. Olfactory neural pathway in mouse hepatitis nasoencephalitis. Acta Neuropathol. **76:**502–506.
6. **Barthold, S. W., and A. L. Smith.** 1987. Response of genetically susceptible and resistant mice to intranasal inoculation with mouse hepatitis virus JHMV. Virus Res. **7:**225–239.
7. **Bartlett, W. P., and G. A. Banker.** 1984. An electron microscopic study of the development of axons and dendrites by hippocampal neurons in culture. I. Cells which develop without intercellular contacts. J. Neurosci. **4:**1944–1953.
8. **Beusch, K. G., and S. E. Malawista.** 1969. Microtubular crystals in mammalian cells. J. Cell Biol. **40:**95–107.
9. **Beushausen, S., and S. Dales.** 1985. In vivo and in vitro models of demyelinating disease. XI. Tropism and differentiation regulate the infectious process of coronaviruses in primary explants of the rat CNS. Virology **141:**89–101.
10. **Binder, L. I., A. Frankfurter, and L. I. Rebhun.** 1985. The distribution of tau in the mammalian central nervous system. J. Cell Biol. **101:**1371–1378.
11. **Bottenstein, J. E., and G. H. Sato.** 1979. Growth of a rat neuroblastoma cell line in serum-free supplemented medium. Proc. Natl. Acad. Sci. USA **76:**514–517.
12. **Caceres, A., G. A. Banker, and L. Binder.** 1986. Immunocytochemical localization of tubulin and microtubule-associated protein 2 during the development of hippocampal neurons in culture. J. Neurosci. **6:**714–722.
13. **Ceccaldi, P. E., J. P. Gillet, and H. Tsiang.** 1989. Inhibition of the transport of rabies virus in the central nervous system. J. Neuropathol. Exp. Neurol. **48:**620–630.
14. **Coulton, P., C. Derbin, P. Kucera, F. LaFay, C. Prehaud, and A. Flamand.** 1989. Invasion of the peripheral nervous system of adult mice by the CVS strain of rabies virus and its avirulent derivative AvO1. J. Virol. **63:**3550–3554.
15. **Dales, S.** 1963. Association between the spindle apparatus and reovirus. Proc. Natl. Acad. Sci. USA **50:**268–275.
16. **Dales, S., and Y. Chardonnet.** 1973. Penetration and uncoating of adenoviruses. Adv. Biosci. **11:**29–40.
17. **Dales, S., K. C. Hsu, and A. Nagayama.** 1973. The fine structure and immunological labelling of the achromatic mitotic apparatus after disruption of cell membranes. J. Cell Biol. **59:**643–655.
18. **Dotti, C. G., and K. Simons.** 1990. Polarized sorting of viral glycoproteins to the axon and dendrites of hippocampal neurons in culture. Cell **62:**63–72.
19. **Dotti, C. G., C. A. Sullivan, and G. A. Banker.** 1988. The establishment of polarity by hippocampal neurons in culture. J. Neurosci. **8:**1454–1468.
20. **Dubois-Dalcq, M., E. W. Doller, M. V. Haspell, and K. V. Holmes.** 1982. Cell tropism and expression of mouse hepatitis viruses (MHV) in mouse spinal cord cultures. Virology **119:**317–331.
21. **Fishman, P. S., J. S. Gass, P. T. Swoveland, E. Lavi, M. K. Highkin, and S. R. Weiss.** 1985. Infection of the basal ganglia by a murine coronavirus. Science **229:**877–879.
22. **Flamand, A., J.-P. Gagner, L. N. Morrison, and B. N. Fields.** 1991. Penetration of the nervous systems of suckling mice by mammalian reoviruses. J. Virol. **65:**123–131.
23. **Gallagher, T. M., S. E. Parker, and M. J. Buchmeier.** 1990. Neutralization-resistant variants of a neurotropic coronavirus are generated by deletions within the amino-terminal half of the spike glycoprotein. J. Virol. **64:**731–741.
24. **Goedert, M., R. A. Crowther, and C. C. Garner.** 1991. Molecular characterization of microtubule-associated proteins tau and MAP2. Trends Neurosci. **14:**193–199.
25. **Knobler, R. L., M. Dubois-Dalcq, M. V. Haspel, A. P. Claysmith, P. W. Lampert, and M. B. A. Oldstone.** 1981. Selective localization of wild type and mutant mouse hepatitis virus (JHM strain) antigens in CNS tissue by fluorescence, light and electron microscopy. J. Neuroimmunol. **1:**81–92.
26. **Kosik, K. S., and E. A. Finch.** 1987. MAP2 and tau segregate into dendritic and axonal domains after elaboration of morphologically distinct neurites: an immunocytochemical study of cultured rat cerebrum. J. Neurosci. **10:**3142–3153.
27. **Kristensson, K., B. Lundh, E. Norrby, L. Payne, and C. Orvell.** 1984. Asymmetric budding of viruses in ependymal and choroid plexus epithelial cells. Neuropathol. Appl. Neurobiol. **10:**209–219.
28. **Kucera, P., M. Dolivo, P. Coulon, and A. Flamand.** 1985. Pathways of the early propagation of virulent and avirulent rabies strains from the eye to the brain. J. Virol. **55:**158–162.
29. **Laemmli, U. K.** 1970. Cleavage of structural proteins during the assembly of the head of bacteriophage T4. Nature (London) **227:**680–685.
30. **LaFay, F., P. Coulon, L. Astic, D. Saucier, D. Riche, A. Holley, and A. Flamand.** 1991. Spread of the CVS strain of rabies virus and of the avirulent mutant AvO1 along the olfactory pathways of the mouse after intranasal inoculation. Virology **183:**320–330.
31. **La Monica, N., L. R. Banner, V. L. Morris, and M. C. Lai.** 1991. Localization of extensive deletions in the structural genes of two neurotropic variants of murine coronavirus JHM. Virology **182:** 883–888.
32. **Lavi, E., P. S. Fishman, M. K. Highkin, and S. R. Weiss.** 1988. Limbic encephalitis after inhalation of a murine coronavirus. Lab. Invest. **58:**31–36.
33. **Lee, G., N. Cowan, and M. Kirschner.** 1988. The primary structure and heterogeneity of tau protein from mouse brain. Science **239:**285–288.
34. **Lee, G., R. L. Neve, and K. S. Kosik.** 1989. The microtubule binding domain of tau protein. Neuron **2:**1615–1624.
35. **Massalski, A., M. Coulter-Mackie, R. L. Knobler, M. J. Buchmeier, and S. Dales.** 1982. In vivo and in vitro models of demyelinating disease. V. Comparison of the assembly of mouse hepatitis virus, strain JHM, in two murine cell lines. Intervirology **18:**135–146.
36. **Matsubara, Y., R. Watanabe, and F. Taguchi.** 1991. Neurovirulence of six different murine coronavirus JHMV variants for rats. Virus Res. **20:**45–58.
37. **Mohandas, D. V., and S. Dales.** 1991. Endosomal association of a protein phosphatase with high dephosphorylating activity against a coronavirus nucleocapsid protein. FEBS Lett. **282:**419–424.
38. **Morris, V. L., C. Tieszer, J. MacKinnon, and D. Percy.** 1989. Characterization of coronavirus JHM variants isolated from Wistar Furth rats with a viral-induced demyelinating disease. Virology **169:**127–136.
39. **Morrison, L. A., R. L. Sidman, and B. N. Fields.** 1991. Direct spread of reovirus from the intestinal lumen to the central nervous system through vagal autonomic nerve fibers. Proc. Natl. Acad. Sci. USA **88:**3852–3856.
40. **Nagayama, A., and S. Dales.** 1970. Rapid purification and immunological specificity of mammalian microtubular paracrystals possessing an ATPase activity. Proc. Natl. Acad. Sci. USA **66:**464–471.
41. **Parham, D., A. Tereba, P. J. Talbot, D. P. Jackson, and V. C. Morris.** 1986. Analysis of JHMV central nervous system infections in rats. Arch. Neurol. **43:**702–708.
42. **Pasick, J. M. M., and S. Dales.** 1991. Infection by coronavirus JHM of rat neurons and oligodendrocyte-type-2 astrocyte lineage cells during distinct developmental stages. J. Virol. **65:**5013–5028.
43. **Perlman, S., G. Jacobsen, and A. Afifi.** 1989. Spread of a neurotropic murine coronavirus into the CNS via the trigeminal and olfactory nerves. Virology **170:**556–560.
44. **Perlman, S., G. Jacobsen, and S. Moore.** 1988. Regional localization of virus in the central nervous system of mice persistently infected with murine coronavirus JHM. Virology **166:**328–338.
45. **Perlman, S., G. Jacobsen, A. L. Olson, and A. Afifi.** 1990. Identification of the spinal cord as a major site of persistence

during chronic infection with a murine coronavirus. Virology **175:**418–426.
46. **Rodriguez-Boulan, E., and S. K. Powell.** 1992. Polarity of epithelial and neuronal cells. Annu. Rev. Cell Biol. **8:**395–427.
47. **Ryder, E. F., E. Y. Snyder, and C. L. Cepko.** 1990. Establishment and characterization of multipotent neural cell lines using retrovirus vector-mediated oncogene transfer. J. Neurobiol. **21:**356–375.
48. **Schuler, G. D., S. F. Altschul, and D. J. Lipman.** 1991. A workbench for multiple alignment construction and analysis. Proteins **9:**180–190.
49. **Skinner, M. A., and S. G. Siddel.** 1983. Coronavirus JHM: nucleotide sequence of the mRNA that encodes nucleocapsid protein. Nucleic Acids Res. **11:**5045–5054.
50. **Sorensen, O., and S. Dales.** 1985. In vivo and in vitro models of demyelinating disease: JHM virus in the rat central nervous system localized by in situ cDNA hybridization and immunofluorescent microscopy. J. Virol. **56:**434–438.
51. **Tooze, J., S. A. Tooze, and S. D. Fuller.** 1987. Sorting of progeny coronavirus from condensed secretory proteins at the exit from the trans-Golgi network of AtT20 cells. J. Cell Biol. **105:**1215–1226.
52. **Tooze, J., S. Tooze, and G. Warren.** 1984. Replication of coronavirus MHV-A59 in sac$^-$ cells: determination of the first site of budding of progeny virions. Eur. J. Cell Biol. **33:**281–293.
53. **Tooze, S. A., J. Tooze, and G. Warren.** 1988. Site of addition of *N*-acetylgalactosamine to the E1 glycoprotein of mouse hepatitis virus-A59. J. Cell Biol. **106:**1475–1487.
54. **Towbin, H., T. Staehelin, and J. Gordon.** 1979. Electrophoretic transfer of proteins from polyacrylamide gels to nitrocellulose sheets: procedure and some applications. Proc. Natl. Acad. Sci. USA **76:**4350–4354.
55. **Tsiang, H., E. Lycke, P.-E. Ceccaldi, A. Ermine, and X. Hirardot.** 1989. The anterograde transport of rabies virus in rat sensory dorsal root ganglia neurons. J. Gen. Virol. **70:**2075–2085.
56. **Tyler, K. L., D. A. McPhee, and B. N. Fields.** 1986. Distinct pathways of viral spread in the host determined by reovirus S1 gene segment. Science **233:**770–774.
57. **Ugolini, G., H. G. J. M. Kuypers, and P. L. Strick.** 1989. Transneuronal transfer of herpes simplex virus from peripheral nerves to cortex and brainstem. Science **243:**89–91.
58. **Vallee, R. B., and G. S. Bloom.** 1991. Mechanisms of fast and slow axonal transport. Annu. Rev. Neurosci. **14:**59–92.
59. **Walsh, E., Y. Ueda, H. Nakanishi, and K. Yoshida.** 1992. Neuronal survival and neurite extension supported by astrocytes co-cultured in trans-wells. Neurosci. Lett. **138:**103–106.
60. **Wang, F.-I., D. R. Hinton, W. Gilmore, M. D. Trousdale, and J. O. Flemming.** 1992. Sequential infection of glial cells by the murine hepatitis virus JHM strain (MHV-4) leads to a characteristic distribution of demyelination. Lab. Invest. **66:**744–754.
61. Wecelewicz, K., K. Kristensson, and C. Orvell. 1990. Segregation of viral structural proteins in cultured neurons of rat spinal ganglia and cord. Neuropathol. Appl. Neurobiol. **16:**357–364.